

Effect of region of interest and slice thickness on vertebral bone mineral density measured by use of quantitative computed tomography in dogs

Yeonho Bae, DVM; Seungjo Park, DVM; Sunghoon Jeon, DVM; Gahyun Lee, DVM; Jihye Choi, DVM, PhD

Objective—To determine the effect of region of interest (ROI) setting and slice thickness on trabecular bone mineral density (BMD) measured with quantitative CT in dogs.

Animals—14 healthy Beagles.

Procedures—CT of the lumbar vertebrae and a quantitative CT phantom was performed. The BMD of trabecular bone was measured from L1 to L7 in 2 ways in all dogs. First, sequential 9.6-mm-thick CT images were acquired and then CT images were reconstructed into transverse CT images with slice thicknesses of 2.4, 4.8, and 9.6 mm. The obtained images were analyzed by circular ROI and trace ROI methods. Second, lumbar vertebrae were scanned with the installed quantitative CT protocol with a slice thickness of 10 mm and then the CT images were analyzed by installed automatic BMD software.

Results—Interclass correlation coefficients of the automatic software (0.975 to 1.0) and the circular method (0.871 to 0.996) were high, compared with those of the trace method (0.582 to 0.996). The BMD measured with the automatic software was not significantly different from that measured with circular ROI and a slice thickness of 9.6 mm. The BMD measured by use of the circular method was not different according to slice thickness.

Conclusions and Clinical Relevance—Results obtained by use of automatic software were similar to those obtained by use of more manual methods. The CT images with thinner slice thickness (2.4 and 4.8 mm) could be used in dogs of toy and small breeds to measure lumbar vertebrae BMD to reduce the limitations of the standard 10-mm slice thickness. (*Am J Vet Res* 2014;75:642–647)

Bone mineral density is the mean concentration of mineral in a bone structure, and osteopenia and osteoporosis are conditions in which BMD is decreased.¹ Quantitative CT and dual energy x-ray absorptiometry have been used to measure BMD in veterinary medicine.^{2,3} Dual energy x-ray absorptiometry has an advantage of lower radiation exposure than quantitative CT, but dual energy x-ray absorptiometry nonselectively incorporates all tissues that x-rays penetrate in a 2-D image. Bone mineral density measured by dual energy x-ray absorptiometry is the sum of densities of soft tissue, trabecular bone, and cortical bone.⁴ Quantitative CT can distinguish between trabecular and cortical bone and measure the BMD of each part separately as a volumetric unit (g/cm^3).²

The precision of measuring BMD with quantitative CT can be affected by apparatus instability, CT slice selection, and ROI selection.⁵ Among them, selection of the CT slice and the ROI setting can be highly in-

ABBREVIATIONS

BMD	Bone mineral density
HU	Hounsfield units
ROI	Region of interest

fluenced by the operator, and operator error is as high as 2.5% to 6% when an entirely manual ROI is used.⁵ Region of interest selection by the operator must be scrutinized because of a potential limit on reproducibility, particularly if different operators are involved in follow-up examinations.⁵ Even if the same shape and size of ROI are used, a small change in position can also result in significantly different values.⁵ Automatic software is used to reduce operator dependence and increase reproducibility when measuring BMD with quantitative CT in human medicine.⁵ When this software is used, the ROI is drawn automatically by use of vertebral anatomic landmarks, and only minor intervention is needed when the ROIs are not suitable for each patient.⁵

Osteopenia and osteoporosis are recognized more often as these abnormalities become more common in the aged population of dogs. Therefore, canine BMD should be estimated and monitored with accurate and reproducible methods. The purpose of the study reported here was to investigate the effect of ROI setting and slice thickness on vertebral trabecular BMDs measured

Received August 7, 2013.

Accepted March 21, 2014.

From the Department of Veterinary Medical Imaging, College of Veterinary Medicine, Chonnam National University, Gwangju, 500-757, South Korea.

Supported by a research grant from Chonnam National University in 2011.

Address correspondence to Dr. Choi (imsono@hanmail.net).

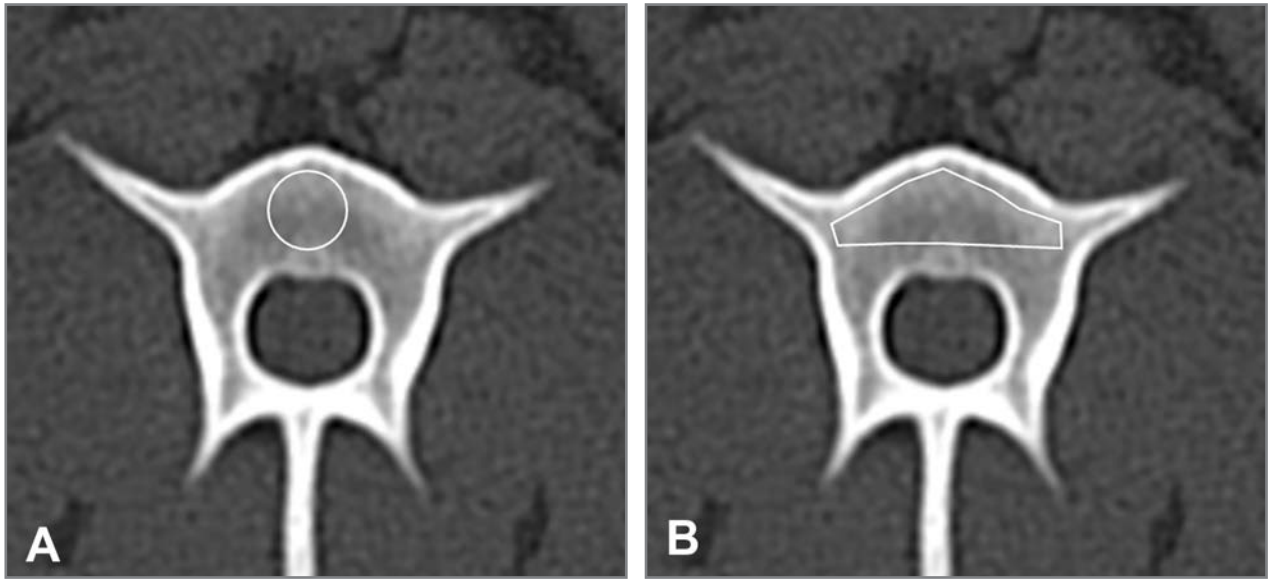


Figure 1—Quantitative CT images of canine lumbar vertebrae obtained with the ROI setting for manual BMD measurements. A—The largest possible circular ROI was drawn with care not to include the cortical bone. B—The tracer ROI was drawn to include the entire trabecular bone except the pedicles.

with quantitative CT in dogs and to compare manual settings and automatic software for the ROI, which was designed for humans, to estimate the applicability of this software to dogs. We hypothesized that the automatic software would have reliability and applicability for setting the ROI for measurement of BMD in canine lumbar vertebrae.

Materials and Methods

Animals—Fourteen healthy research Beagles (10 males and 4 females), 1 to 2 years of age, with a body weight ranging from 9.6 to 11.22 kg (median, 10.41 kg), were used in this study. The dogs were housed in individual cages and received commercial food and tap water ad libitum. All dogs were deemed healthy on the basis of results of a physical examination, CBC, serum biochemical analyses (activities of alkaline phosphatase, alanine aminotransferase, and amylase and concentrations of albumin, calcium, cholesterol, creatinine, glucose, phosphate, total bilirubin, total protein, and BUN), electrolyte analysis (sodium, potassium, and chloride), urinalysis, radiography, and abdominal ultrasonography. Hormone analysis results for thyroxine, free thyroxine, and resting plasma cortisol concentrations were within reference ranges. This animal study protocol was approved by the Institutional Animal Care and Use Committee of Chonnam National University, and the animals were cared for in accordance with the Guidelines for Animal Experiments of Chonnam National University.

CT scans—All dogs were used twice, in turn, at 1-week intervals. Food was withheld for at least 24 hours prior to the CT examinations. After induction of anesthesia with a combination of zolazepam-tiletamine^a (2.5 mg/kg, IM) and medetomidine^b (0.05 mg/kg, IM), CT images were acquired with a 16-channel multidetector CT scanner^c with the dog in dorsal recumbency. To exclude the

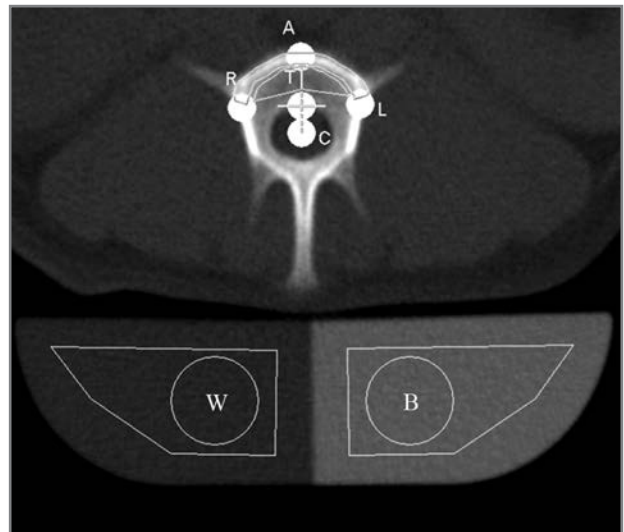


Figure 2—Quantitative CT image of a canine lumbar vertebra obtained with the ROI drawn by use of automatic software. Notice the ROI on the vertebra, the water equivalent phantom (W), and the bone equivalent phantom (B). The vertebral ROI was confined to trabecular bone by use of the vertebral canal, ventral point of the vertebral body, bilateral intermediate points of the vertebral body, and the ventral point of the vertebral canal as landmarks. A = Ventral point of the vertebral body. C = Center of the vertebral canal. L = Left intermediate point of the vertebral body. R = Right intermediate point of the vertebral body. T = Ventral point of the vertebral canal.

effect of table height on BMD, table height was fixed to 125 mm for all scanning procedures. A quantitative CT phantom^d was placed on the CT scanner table for reference. Lateral topograms were obtained covering the area from T12 to the sacrum to define appropriate vertebral levels and determine the angles for subsequent CT scans. Then, CT images were acquired from L1 to L7 in 2 ways in all dogs. First, sequence CT images were acquired with collimator width of 9.6 mm at 130 kVp and 100 mAs with the transverse section of each vertebral body parallel to

the cranial and caudal endplates with or without a tilted gantry, and then CT images were reconstructed into slice thicknesses of 2.4, 4.8, and 9.6 mm with a standard bone reconstruction algorithm on a 120-mm field of view. Second, lumbar vertebrae were scanned with the installed quantitative CT protocol^e (80 kVp and 24 mAs with a slice thickness of 10 mm in sequence). The CT image was positioned at the center of the vertebral body, and the angle of each CT image was corrected to be parallel to each endplate with or without a tilted gantry.

Image analysis—All CT images were evaluated separately at a workstation by 2 operators (BYH and PSJ) at a window width of 1,500 HU and a window level of 450 HU. The manual BMD measurements were performed in sequential CT images with slice thicknesses of 2.4, 4.8, and 9.6 mm. In CT images with thinner slice thicknesses, such as 2.4 and 4.8 mm, more cranial CT slices from the center of a vertebral body were selected to exclude the basivertebral vein, located at the center of a vertebral body. The radiopacity of each lumbar vertebra was measured with circular and tracer ROIs. The largest circular ROI was drawn with care not to include the cortical bone and basivertebral vein, and the tracer ROI was drawn including the entire trabecular bone except the pedicle (Figure 1). Each ROI was drawn every time by each operator separately. Phantom density was measured on the same image, and the measured trabecular radiopacity was converted to BMD by use of the following equation.⁴

$$\text{BMD} = 200 t / (b - w)$$

where *t* is the radiopacity (in HU) of measured trabecular bone, *b* is the radiopacity (in HU) of 200 mg/cm³ for the calcium hydroxyapatite phantom, and *w* is the radiopacity (in HU) of 0 mg/cm³ for the calcium hydroxyapatite phantom.

The ROI was automatically drawn on the trabecular bone by the software by use of vertebral landmarks such as the vertebral canal, the ventral point of the vertebral body, bilateral intermediate points of the vertebral body, and the ventral point of the vertebral canal as well as the bone and water portion of the phantom for reference (Figure 2). Each operator intervened to reposition inappropriate ROIs to appropriate landmarks considering vertebral anatomy.

Statistical analysis—Analysis of reproducibility between operators was performed with the interclass correlation coefficient test. Analysis of variance was used to investigate differences among slice thicknesses of images and among vertebrae. The Student *t* test was used to determine differences between the automatic software measurement and the measurements obtained by use of the circular ROI method. The Mann-Whitney *U* test was performed to analyze the sex-related difference between groups because the female group was small and did not have a normal distribution. The level of significance was set at *P* < 0.05. Statistical analysis was performed with statistical software.^f

Results

A total of 1,470 lumbar vertebral CT images from 14 dogs were acquired: 1 image from each vertebra by use of automatic software, and 2, 4, and 8 images from each vertebra in a slice thickness of 9.6, 4.8, and 2.4 mm, respectively. The CT images obtained from 5 lumbar vertebrae with spondylosis deformans in 2 female dogs were excluded. Then, 372 images were analyzed after selecting only 1 CT image in each slice thickness.

The automatic software algorithm was successfully applied with fully automatic performance in 28.57% of the CT images. The operator intervened for the rest to set up the landmarks because of inaccurate positioning of vertebral landmarks caused by interference by ribs, the transverse process, and the ilium (Figure 3). After manual intervention, the trabecular BMD was measured successfully.

Interoperator reproducibility was high for the automatic software measurement (interclass correlation coefficient, 0.975 to 1) and the circular method (interclass correlation coefficient, 0.871 to 0.996; Figure 4). However, the trace ROI had relatively lower reproducibility on CT images (interclass correlation coefficient, 0.582 to 0.996) in L1, L4, and L5 with a slice thickness of 2.4 mm, L5 with a slice thickness of 4.8 mm, and L6 with a slice thickness of 9.6 mm. Because of low reproducibility, the data obtained with the trace method were excluded from further statistical analysis. The trabecular BMD measured with the automated software and the circular ROI in each lumbar vertebra for males and females were determined (Tables 1 and 2). Trabec-

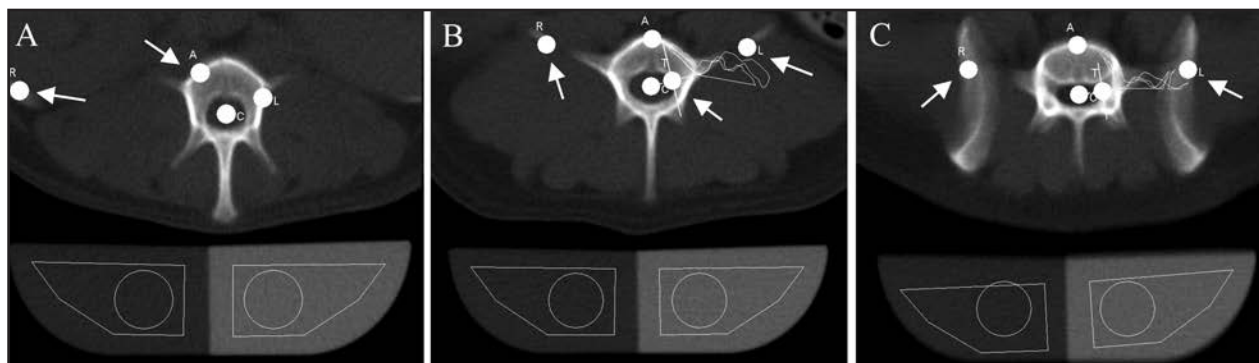


Figure 3—Quantitative CT images of canine lumbar vertebrae obtained by use of automatic software, which resulted in errors in placement of vertebral landmarks caused by the ribs (A), transverse process (B), and ilium (C). Arrows indicate incorrect placement of the vertebral landmarks for the ROI. See Figure 2 for remainder of key.

ular BMD did not appear to be substantially different according to sex, although the number of female dogs was too small for statistical analysis.

Bone mineral density of each lumbar vertebra in male dogs, measured on CT images with the automatic software (slice thickness, 10 mm), was not significantly different from those measured with the circular method (slice thickness, 9.6 mm; Table 1). Both methods typically yielded similar BMD in female dogs; however, the number of CT images obtained from female dogs was too small to analyze statistically. Trabecular BMD measured with the circular method in images was analyzed for diversity according to slice thickness (2.4, 4.8, and 9.6 mm). No significant difference in BMD was observed in male dogs according to CT images with various slice thicknesses (Figure 5).

Bone mineral density of each individual lumbar vertebra was not significantly different when measured by use of the circular and automatic software measure-

ment methods. Mean trabecular BMD in male Beagles, measured with the circular ROI in 9.6-mm-thick lumbar CT images, was 275.97 mg/cm³ (range, 268.48 to 282.88 mg/cm³).

Discussion

Decreased bone mass in cases of osteopenia and osteoporosis has been widely studied in human medicine because this condition can cause serious disorders such as fractures with aging.¹ However, the prevalence of osteopenia or osteoporosis in dogs is considerably lower than that in humans⁶ and the necessity for measuring BMD is relatively underestimated. However, the typical lifespan of dogs has increased and geriatric diseases that may influence BMD are increasing; also, hyperadrenocorticism is more common in dogs than human patients, and this endocrine disease decreases BMD.⁷ Therefore, a standardized system for measuring BMD is needed in dogs.

The vertebrae consist of mainly trabecular bone in the vertebral body and mainly compact bone in the endplates, pedicles, and cortical bone regions.⁸ Trabecular bone is more susceptible to early bone loss because the metabolic turnover rate of trabecular bone is 4 to 8 times that of cortical bone.⁴ Thus, the vertebral body is commonly used for BMD.^{1,8}

Quantitative CT is the most sensitive and accurate noninvasive method to evaluate BMD, and this modality discriminates cortical bone from trabecular bone and measures their BMDs separately.⁹ Bone mineral density measured by quantitative CT is volumetric data; therefore, these data are closest to the true bone mass. A calibration phantom used in quantitative CT as a reference is composed of a solid compound for the water equivalent and calcium hydroxyapatite for the bone equivalent. The radiopacities of bone are converted to BMD by use of a mathematical formula based on the radiopacities of water and the bone equivalent parts of the phantom.^{4,10} In the present study, the dogs and a phantom were scanned at the same time so as not to be affected by variations in scanning protocol.

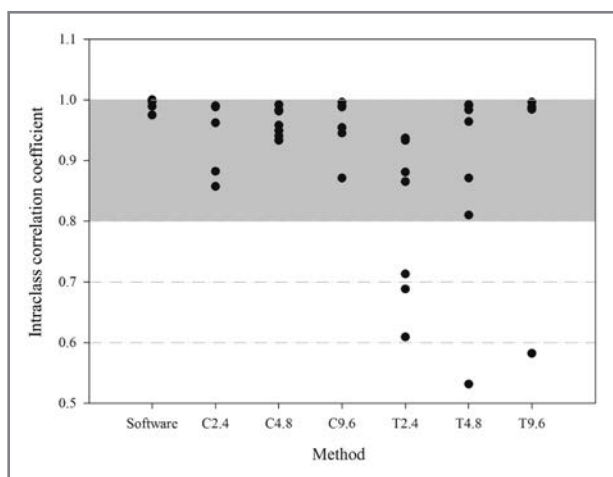


Figure 4—Intraclass correlation coefficients for CT images of canine vertebrae with ROI obtained with slice thicknesses of 2.4, 4.8, and 9.6 mm by use of automatic software, a circular ROI method (C2.4, C4.8, and C9.6, respectively), or a trace method (T2.4, T4.8, and T9.6, respectively). Shaded area indicates high intraclass correlation coefficients.

Table 1—Mean \pm SD trabecular BMDs (mg/cm³) of lumbar vertebrae (L1 to L7) of male dogs (n =10) obtained by use of CT with automatic software and circular ROI methods.

Method	L1	L2	L3	L4	L5	L6	L7
Software	261.4 \pm 23.3	257.7 \pm 22.27	262.6 \pm 22.16	260.4 \pm 29.33	254.5 \pm 31.32	248.8 \pm 26.68	259.4 \pm 25.49
C2.4	290.2 \pm 25.66	286.1 \pm 29.72	288.5 \pm 21.99	291.9 \pm 29.25	274.3 \pm 39.81	257.3 \pm 34.97	276.2 \pm 22.45
C4.8	297.8 \pm 29.14	289.1 \pm 25.7	291.5 \pm 21.14	290.4 \pm 32.54	277.9 \pm 37.84	266.2 \pm 33.62	283.1 \pm 28.53
C9.6	283 \pm 29.57	278.9 \pm 28.63	282.3 \pm 28.68	281.1 \pm 39.34	271.1 \pm 37.37	259.2 \pm 30.1	276.2 \pm 20.42

C2.4 = Circular ROI method with a slice thickness of 2.4 mm. C4.8 = Circular ROI method with a slice thickness of 4.8 mm. C9.6 = Circular ROI method with a slice thickness of 9.6 mm.

Table 2—Mean \pm SD trabecular BMDs (mg/cm³) of lumbar vertebrae (L1 to L7) of female dogs (n =4) obtained by use of CT with automatic software and circular ROI methods.

Method	L1	L2	L3	L4	L5	L6	L7
Software	263.1 \pm 16.35	256.1 \pm 11.03	252.4 \pm 9.57	255.2 \pm 1.75	248.9 \pm 14.04	240.7 \pm 20.43	261 \pm 19.48
C2.4	281.7 \pm 22.08	273.3 \pm 17.11	278.5 \pm 16.69	276.7 \pm 7.76	294.4 \pm 28.73	271.9 \pm 26.44	270.1 \pm 11.98
C4.8	290.7 \pm 16.56	293.5 \pm 17.32	294.4 \pm 16.96	282 \pm 8.58	303 \pm 20.86	281.2 \pm 29.44	279.2 \pm 1.11
C9.6	277 \pm 16.34	273.3 \pm 6.68	277.6 \pm 5.73	277.6 \pm 12.33	285.4 \pm 20.08	263.9 \pm 24.88	274.8 \pm 7.16

See Table 1 for key.

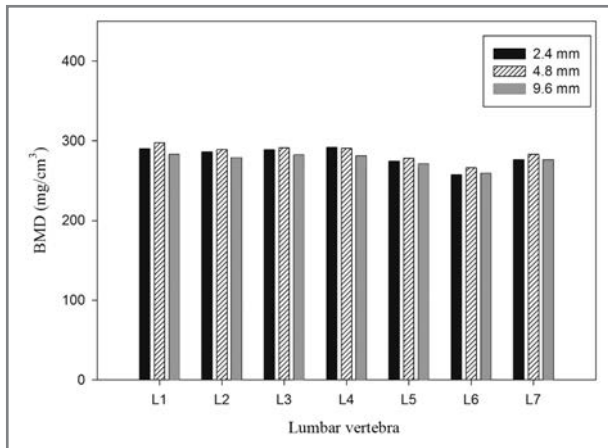


Figure 5—Mean values of BMD measured with a circular ROI at slice thicknesses of 2.4, 4.8, and 9.6 mm in lumbar vertebrae in 10 male dogs.

The automatic software consisted of a scanning part and an analysis part.⁹ In the scanning part, a CT image sequence with a slice thickness of 10 mm was obtained. In the analysis part, an ROI was automatically selected to encompass the trabecular bone on the basis of a vertebral landmark, and BMD (in mg/cm^3) was measured. These processes are almost fully automated in human medicine, with a success rate $> 90\%$.⁵ In contrast, the success rate of fully automatic performance in the present study was only 28.57%, and an operator's manual intervention was needed for many of the CT images. The reason for the low success rate could be that trabecular BMD was measured from all lumbar vertebrae including the caudal lumbar region, whereas BMD was measured from T12 to L4 in a previous study¹¹ in humans. Computed tomography images of L7 contained iliac wings, which interfere with the landmark for the ROI in dogs; thus, operator intervention was required for all CT images of L7. Ribs were displaced with lumbar vertebra in the cranial lumbar CT images, which led to chances for errors in the automatic ROI setting in dogs because a dog's thorax is smaller than that of a human. In addition, the vertebral body of a dog is wide, unlike the round shape of a human's vertebral body,² and this morphological difference may cause perturbations in the automatic algorithm. However, the automatic software measurement was performed successfully after manual intervention, and this method had promising interoperator reproducibility; therefore, the failure of fully automatic performance in some CT images did not influence the accuracy of measuring trabecular BMD by use of the automatic software in dogs. The automatic software measurement was completed with 1-click processing on fully automatic performance. The manual intervention was performed during a few seconds. However, manual measurements, especially the tracer ROI method, required more time than automatic software measurement because ROIs must be manually set over the vertebrae as well as the phantom and the BMD must be manually calculated from radiopacities with a conversion equation. The manual methods were more time-consuming than automatic software measurement, although the exact time

required was not determined for BMD measurement in the present study.

The circular and trace ROI methods were applied as manual methods. The circular ROI is the most reproducible method¹²; therefore, the circular method was used as the gold standard to estimate the reliability of the automatic software in this study. The trace ROI defined the trabecular bone as large as possible; a similar-shaped ROI was confirmed by use of the automatic software.¹³ The reproducibility of the automatic software measurement and the circular method was greater than that of the trace method. Trabecular bone was defined by a mathematical algorithm in the automatic software in which the border between cortical and trabecular bone was determined at the region where the radiopacity decreased to 60% of that of cortical bone.⁵ Then, the ROI confirming the trabecular bone was drawn with a constant distance from the border.⁵ However, no clear line of discrimination was observed between cortical bone and trabecular bone when the trace method was used, and this division was performed by visual inspection. In the present study, there was no significant difference between methods, although the median BMDs obtained by use of the circular method were greater than those obtained by use of the software method. Similar to the trace method, no clear line of discrimination was observed between cortical bone and trabecular bone when circular method was used. It was considered that focal hyperdense areas of trabecular bone or beam hardening areas were included in the circular ROI and resulted in higher BMDs in the circular ROI.

A 10-mm-thick axial slice in the vertebral midsection is recommended for vertebral BMD analysis in humans.⁹ However, dogs have a variety of vertebral sizes according to breed and body size. Therefore, a thinner slice thickness is needed for vertebral BMD analysis in toy- and small-breed dogs. Furthermore, the prevalence of hyperadrenocorticism, which is an endocrine disease that causes a decrease in BMD, is higher in small-breed dogs than that in large-breed dogs.¹⁴ We realize the necessity of measuring BMD in clinical practice, particularly in older small-breed dogs. Similarly, slice images < 10 mm thick are selected to measure infant BMD in human medicine because infant lumbar length is approximately 43 mm.² In thinner slice images, the signal-to-noise ratio decreases and affects radiopacity measurement. An appropriately sized ROI should be applied to a CT image according to slice thickness to reduce this problem. In a previous *in vitro* study¹⁵ that used a phantom, an analogous coefficient of variation was acquired when the appropriate ROI was used; an ROI > 11 mm² is needed for CT images with a slice thickness of 1 mm, an ROI > 5 mm² is needed for a slice thickness of 3 mm, and an ROI > 3 mm² is needed for a slice thickness of 5 mm. Signal-to-noise ratio is irrelevant to the size of the ROI when a slice thickness > 10 mm is used.¹⁵

When a thinner slice is used, radiopacities change with histologic variations in trabecular bone because quantitative CT calculates the mean of radiopacities of the inner region of the slice volume.¹⁶ This means that even focal variation can strongly affect the radiopacities in images with a thinner slice thickness. Therefore, use of appropriate and valid slice thickness is important for an accurate measurement.

In the present study, CT images with slice thicknesses of 2.4 and 4.8 mm were reconstructed and the values were compared with those of CT images with a slice thickness of 9.6 mm. No significant differences in BMD were observed among CT images with each slice thickness when the circular method was used. We speculate that an appropriate and valid ROI may minimize the signal-to-noise ratio variation despite use of a thinner slice thickness.¹⁵ Appropriate selection of CT images that did not contain the basivertebral vein was also considered to minimize the effect of anatomic variation in the images obtained with a slice thickness of 2.4 or 4.8 mm. Consequently, thinner CT images can be used confidently for measuring BMD by means of quantitative CT in toy- or small-breed dogs if accompanied by the appropriate ROI size and CT image selection.

The trabecular BMD in individual lumbar vertebrae was uniform in this study. This result was contrary to findings in a previous study¹⁷ that used dual energy x-ray absorptiometry that lumbar BMD was different according to the anatomic location. However, BMD measured with dual energy x-ray absorptiometry can be affected by cortical BMD and the summation of soft tissue and calcified material such as the spinous processes of vertebrae, intestinal materials, and aortic calcification because this modality is unable to separate trabecular from cortical bone.⁹

No substantial difference was observed in the BMD between males and females, even though the number of female dogs was too small to statistically analyze. In general, human males have higher BMD than do females.^{1,18,19} Bone mineral density in dogs increases until 6 years of age and then decreases slightly.¹⁹ This change of BMD has also been observed in humans, in which BMD increases until peak bone mass occurs in adolescence.²⁰ We assumed no difference in BMD between sexes because the typical age of dogs used in this study was 1 to 2 years and none of the dogs had reached peak bone mass. Further study is necessary with female and male dogs of various ages.

The applicability of use of the automatic software for measuring canine trabecular BMD density in lumbar vertebra of dogs was confirmed. Furthermore, the reliability of BMD measurements in CT images with thinner slices was verified, suggesting that the 10-mm limitation of standard slice thickness in toy- and small-breed dogs can be reduced. Our results will be useful to establish the foundation of a reliable method for canine BMD measurements by means of quantitative CT and also provide basic BMDs for investigating osteopenia and osteoporosis in dogs.

- a. Zoletil, Virbac, Carros, France.
- b. Domitor, Orion Corp, Espoo, Finland.
- c. Siemens Emotion 16, Siemens, Forchheim, Germany.

- d. Calcium hydroxyapatite rod (0 and 200 mg/cm³), Siemens, Forchheim, Germany.
- e. Syngo Osteo CT, Siemens, Forchheim, Germany.
- f. SPSS Statistics, version 20, IBM Corp, Armonk, NY.

References

1. Cummings SR, Bates D, Black DM. Clinical use of bone densitometry. *JAMA* 2002;288:1889–1897.
2. Braillon PM, Lapillonne A, Ho PS, et al. Assessment of the bone mineral density in the lumbar vertebrae of newborns by quantitative computed tomography. *Skeletal Radiol* 1996;25:711–715.
3. Norrdin RW, Carpenter TR, Hamilton BF, et al. Trabecular bone morphometry in Beagles with hyperadrenocorticism and adrenal adenomas. *Vet Pathol* 1988;25:256–264.
4. Cheon H, Choi W, Lee Y, et al. Assessment of trabecular bone mineral density using quantitative computed tomography in normal cats. *J Vet Med Sci* 2012;74:1461–1467.
5. Klotz E, Kalender WA, Sandor T. Automated definition and evaluation of anatomical ROIs for bone mineral determination by QCT. *IEEE Trans Med Imaging* 1989;8:371–376.
6. Turner AS. Animal models of osteoporosis—necessity and limitations. *Eur Cell Mater* 2001;1:66–81.
7. Bertagna X, Guignat L, Groussin L, et al. Cushing's disease. *Best Pract Res Clin Endocrinol Metab* 2009;23:607–623.
8. Genant HK, Block JE, Steiger P, et al. Quantitative computed tomography in assessment of osteoporosis. *Semin Nucl Med* 1987;17:316–333.
9. Guglielmi G, Schneider P, Lang TF, et al. Quantitative computed tomography at the axial and peripheral skeleton. *Eur Radiol* 1997;7:S32–S42.
10. Kalender WA, Suess C. A new calibration phantom for quantitative computed tomography. *Med Phys* 1987;14:863–866.
11. Kalender WA, Brestowsky H, Felsenberg D. Bone mineral measurement: automated determination of midvertebral CT section. *Radiology* 1988;168:219–221.
12. Breatnach E, Robinson PJ. Repositioning errors in measurement of vertebral attenuation values by computed tomography. *Br J Radiol* 1983;56:299–305.
13. Banks LM, Stevenson JC. Modified method of spinal computed tomography for trabecular bone mineral measurements. *J Comput Assist Tomogr* 1986;10:463–467.
14. Peterson ME. Diagnosis of hyperadrenocorticism in dogs. *Clin Tech Small Anim Pract* 2007;22:2–11.
15. Lee JY, Kim KD, Park CS. Effect of the slice thickness and the size of region of interest on CT number. *Korean J Oral Maxillofac Radiol* 2001;31:85–91.
16. Fukuda S, Iida H. Effects of orchidectomy on bone metabolism in Beagle dogs. *J Vet Med Sci* 2000;62:69–73.
17. Zotti A, Isola M, Sturaro E, et al. Vertebral mineral density measured by dual-energy x-ray absorptiometry (DEXA) in a group of healthy Italian Boxer dogs. *J Vet Med A Physiol Pathol Clin Med* 2004;51:254–258.
18. Lauten SD, Cox NR, Brawner WR, et al. Use of dual energy x-ray absorptiometry for noninvasive body composition measurements in clinically normal dogs. *Am J Vet Res* 2001;62:1295–1301.
19. Martin RK, Albright JP, Jee WS, et al. Bone loss in the Beagle tibia: influence of age, weight, and sex. *Calcif Tissue Int* 1981;33:233–238.
20. Boot AM, de Ridder MA, Pols HA, et al. Bone mineral density in children and adolescents: relation to puberty, calcium intake, and physical activity. *J Clin Endocrinol Metab* 1997;82:57–62.